# Rotational Spectrum and Intramolecular Hydrogen Bonding in 1,2-Butanedithiol

Marcos Juanes,[a] Rizalina Tama Saragi,[a] Yan Jin,[a,1] Oliver Zingsheim,[b] Stephan Schlemmer,[b] Alberto Lesarri[a,c]*

[a]Departamento de Química Física y Química Inorgánica, Facultad de Ciencias, Universidad de Valladolid, Paseo de Belén 7, 47011 Valladolid (Spain)

[b]I. Physikalisches Institut, Universität zu Köln, Zuelpicher Strasse 77, 50937 Köln (Germany)

[c]I.U. CINQUIMA, Universidad de Valladolid, Paseo de Belén, 7, 47011 Valladolid (Spain)

*Corresponding author: Prof. Dr. Alberto Lesarri, lesarri@qf.uva.es

KEYWORDS: Thiols, Rotational spectroscopy, Supersonic jet spectroscopy, Intramolecular hydrogen bonding, Sulfur hydrogen bonding, Molecular structure,

[1] Permanent address: School of Chemistry and Chemical Engineering, Chongqing University, Daxuecheng South Rd. 55, 401331, Chongqing, China

**ABSTRACT**

The jet-cooled rotational spectrum of 1,2-butanedithiol was observed in the frequency region 2-8 GHz. Two conformers were detected for the molecule, corresponding to trans- and gauche-carbon molecular skeletons, both sharing a gauche arrangement of the two thiol groups. The structural analysis included a ground-state effective structure, isotopic substitution coordinates, B3LYP-D3(BJ) density functional molecular orbital calculations and non-covalent interactions mapping with NCIPlot. The structural data confirm that the two thiol groups synchronize their orientation either parallel or antiparallel to support intramolecular S-H···S weak hydrogen bonding, reminiscent of the intramolecular hydrogen bond networks observed with adjacent alcohol groups. DFT calculations on 1,2-butanediol and 1,2-ethanedithiol offered structural comparisons with the title compound.

## INTRODUCTION

High-resolution rotational studies of thiols (R-S-H, R = organic) and selenols (R-Se-H) have attracted much less attention than alcohols, despite the chemical and biological relevance of these functional groups. The three organocompounds nominally share the same connectivity, but their electronic differences result in smaller bond dissociation energies [1], longer calchogen-hydrogen and carbon-calchogen bonds and R-S-H deviations close to right angles. In particular, the larger atomic size, smaller electronegativity and high polarizability of sulfur and selenium strongly affect their capacity to form intra- and intermolecular hydrogen bonds [2]. The interest and characteristics of sulfur-centered hydrogen bonds have been reviewed by Biswal and Wategaonkar [3,4], using laser spectroscopy and computational Chemistry tools.

Rotational spectroscopy offers a direct route to the gas-phase structure through the molecular moments of inertia, providing experimental information and validation of computational models on free isolated molecules [5]. Additionally, the combination of microwave spectroscopy and internally cooled supersonic jets offers the possibility to generate, stabilize and probe weakly-bound aggregates and to analyze the interaction forces [5,6,7]. To date, rotationally resolved investigations of thiols and related sulfides have included mostly small alkyl derivatives like ethanethiol [8], ethanedithiol [9], propanethiol [10], propanedithiol [11], 3-butene-1-thiol [12], 3-butyne-1-thiol [13], cyclopropanemethanethiol [14], mercaptoacetonitrile [15], furfuryl mercaptane [7], diethyldisulfide [16], diallyldisulfide [17] and diphenyldisulfide [18]. For selenols, the 2-propene [19], 3-butene [20], 3-butyne [21], cyclopropylmethyl [22] and propargyl [23] derivatives have been studied. In presence of several polar groups some of these compounds offer the possibility of structurally analyzing thiol or selenol intramolecular hydrogen bonding, like (S/Se)-H···(S/Se) [9,11] or (S/Se)-H···$\pi$ [12-14,19-23]. When thiol/selenol groups are present in adjacent atoms intramolecular hydrogen bonds may contribute significantly to molecular stabilization, as in diols [24,25,26]. It may be hypothesized that these

interactions could eventually be extended to form intramolecular hydrogen bonding networks, as observed in poliols like the monosaccharides [27,28]. Globally, the information on intramolecular hydrogen bonding is highly complementary to that obtained from intermolecular interactions on isolated clusters, contributing to our understanding of long-range non-covalent interactions in the gas phase.

In this work we report on the rotational spectrum, molecular structure and intramolecular hydrogen bonding of 1,2-butanedithiol. The molecule compares directly with 1,2-butanediol [25], where all six observed isomers exhibit an intramolecular O-H···O hydrogen bond. Will the exchange of the two oxygen atoms by sulfur affect the molecular conformation and hydrogen bonding? We address this problem using pulsed-jet chirped-pulsed Fourier transform microwave spectroscopy (CP-FTMW) in the cm-wave region (2-8 GHz). The introduction of CP-FTMW by Pate [29,30] achieves effective multiplexing in the microwave region, allowing routine broadband operation and excellent sensitivity. The experimental data were rationalized with molecular orbital calculations.

## EXPERIMENTAL AND COMPUTATIONAL METHODS

A sample of 1,2-butanedithiol (>97% GC) was obtained commercially and used without further purification. The sample was heated inside a reservoir nozzle (35°C) to ensure sufficient vapor pressure (b.p. 77°C at 37 hPa), co-expanding with a stream of pure neon at backing pressures of 0.25 MPa. A single nozzle with a circular orifice of 0.8 mm was used for preparation of the pulsed jet (typically 900 μs), propagating perpendicularly to the emitting and receiving horn antennas. The expansion chamber was evacuated with an oil diffusion pump to ultimate pressures of $10^{-7}$ hPa. The chirped-pulsed Fourier transform microwave (CP-FTMW) spectrometer uses a direct-digital design following Pate [30]. In this experiment, the jet was probed with short (1 μs) chirped-pulses covering the bandwidth of 2-8 GHz, using a sequence of 4 microwave pulses per molecular pulse. The chirped-pulse was amplified to a nominal power of 20 W and radiated into the jet. Detection of the transient emission resulting from rotational decoherence used a digital oscilloscope (20 MSamples/s) and extended for 40 μs per excitation pulse. The Fourier transformation used a Kaisser-Bessel window [31], producing linewidths of ca. 100 kHz. For the present purposes ca. 1 M averages were acquired at a repetition rate of 5 Hz.

Computational methods complemented the experimental work. For this purpose we compared the B3LYP density functional (DFT) method (with inclusion of Grimme's D3 empirical dispersion corrections [32]) and second-order Møller-Plesset perturbation theory (MP2). Both calculations used Ahlrich's def2-TZVP basis set [33] and were conducted with Gaussian16 [34]. Frequency calculations used the same level of theory and the harmonic approximation. The presence of non-covalent interactions (NCI) in the molecule was analyzed with the NCIPLOT methodology, based on a reduced gradient of the electronic density [35].

## RESULTS AND DISCUSSION

*Rotational spectrum*

The conformational landscape of 1,2-butanedithiol is similar to the diol analogue, discussed by Melandri [25]. Briefly, the open-chain molecule contains four independent internal rotors, which may generate $3^4$=81 staggered orientations, chemically assumed to be more stable. Additionally, all observed diols exhibit intramolecular hydrogen bond stabilization [24-26], which could also happen in the dithiol favoring specific species. In order to quantify the structural preferences of 1,2-butanedithiol a conformational search was started without any geometrical constrain, using both DFT (B3LYP-D3(BJ)) and ab initio (MP2) methods. The calculations were followed by vibrational frequency calculations to obtain the force field and centrifugal distortion contributions. The results in Table 1 show eight conformers predicted below 5 kJ mol$^{-1}$, which a priori could be observable in the jet expansion. For comparison purposes the different isomers were labelled as in 1,2-butanediol [25], i.e. with dihedrals $\tau_1$ (H-S(1)-C(1)-C(2)), $\tau_2$ (S(1)-C(1)-C(2)-S(2)), $\tau_3$ (C(1)-C(2)-C(3)-C(4)) and $\tau_4$ (C(1)-C(2)-S(2)-H), using +/-gauche (G/G') and anti (A) indicators depending on the dihedral values (capital letters for the heavy atom dihedrals, smaller letters for the hydrogen orientations). For convention, the compound was assumed to display (2)-R stereochemistry, the two enantiomers being indistinguishable in conventional single-photon transition spectroscopy [36].

The spectrum in Figure 1 was surveyed attending to the predicted conformational energies. Intense $\mu_a$ R-branch transitions were detected for a first species denoted isomer 1, and later extended to additional $\mu_b$ and $\mu_c$ transitions. The present experimental dataset comprised 48 transitions with angular momentum quantum numbers $J$=0-8 ($K_{-1}$=0-2). The spectral analysis used a standard semirigid rotor Watson's S-reduced Hamiltonian ($I^r$ representation), since no hyperfine effects were noticeable. In particular, the internal rotation of the terminal methyl group did not produce observable tunneling effects. In addition to the rotational constants,

three quartic centrifugal distortion constants were determined for isomer 1 using Pickett's program CALPGM [37], with a satisfactory rms microwave deviation of the fit of 5 kHz (mean correlation coefficients below 0.26). A small set of (6-11) rotational transitions was later measured for each of the six monosubstituted $^{13}C$ and $^{34}S$ isotopologues in natural abundance (1-4%), providing inertial data for the structural analysis. Further investigation of the spectrum revealed a second conformation denoted isomer 2, with dominant (Q- and R-branch) $\mu_b$ spectrum and a small number of additional $\mu_a$ and $\mu_c$ transitions. The spectral dataset comprised in this case 34 transitions ($J$=0-6, $K_{-1}$=0-5), which similarly allowed the determination of the rotational constants and four centrifugal distortion coefficients. The quality of the fit was similar (rms mw deviation of 5 kHz and mean correlation coefficients below 0.31). For isomer 2 only the two $^{34}S$ monosubstituted isotopologues could be measured in natural abundance. The spectroscopic parameters for conformers 1 and 2 and their isotopic species are shown in Tables 2 and 3, respectively. The full set of frequency measurements are found in the Supporting information (Tables S1-S10).

*Molecular structure*

The structural analysis used the effective and substitution methods, described elsewhere [38]. The ground-state effective structures resulted from a least-squares fit of the experimental moments of inertia to selected independent structural parameters, as implemented in Rudolph's RU212 program [39]. For conformer 1 we fitted 21 inertial data (7 isotopologues) to all parameters defining the heavy-atom skeleton (5 bond distances, 4 valence angles and three dihedrals). The derived structure reproduced the experimental rotational constants below 0.2 MHz (rms residual of 66 kHz and rms correlation coefficient of 0.50). For conformer 2, the 9 inertial data were used initially to fit 4 valence angles and 3 dihedrals, but this fit did not converge. We then fitted the valence angles and used the results to fit the dihedrals separately. This fit reproduced the observed rotational constants below 0.4 MHz (rms residual of 280 kHz

and rms correlation coefficient of 0.40). The effective structures of conformers 1 and 2 are collected in Tables 4 and 5, while the fit residuals are presented in Tables S11-S12 (Supplementary information). For both conformers the hydrogen atom positions were fixed to the B3LYP-D3(BJ) structure, which better reproduces the rotational constants. The atomic coordinates can be compared with the computational predictions in Tables S13-S14 (Supplementary information).

Additionally, the substitution coordinates of Tables S15-S16 (Supplementary information) were calculated using the Kraitchman equations [38] and Costain errors [40]. This method produced a partial substitution structure for conformer 1, also reported in Table 4. However, one of the coordinates of the sulfur atom S(2) results undeterminable [41], reducing the accuracy of the substitution structure (as observed in the differences between *r*(C(1)-S(1)) and *r*(C(2)-S(2) and the discrepancy with the predicted values).

The structural information obtained from the isotopic data clearly identifies the most intense conformer 1 of 1,2-butanedithiol as isomer gG'Ag', consistently predicted in Table 1 as the global minimum. Conformer gG'Ag' displays a heavy atom skeleton similar to the aG'Ag global minimum of 1,2-butanediol [25], i.e. an all-trans (A) carbon configuration with negative-gauche (G') orientation of the two sulfur hydrogens. Conversely, the hydrogen atoms in 1,2-butanedithiol are oriented gg' instead of the ag orientation in 1,2-butanediol. The presence of several conformers sharing the heavy-atom skeleton but differing in the orientation of the terminal hydrogen atoms, which synchronize to maintain the intramolecular hydrogen bonding, is characteristic of molecules with multiple alcohol groups and has been observed repeatedly in gas-phase studies, as in monosaccharides [27,28]. The hydrogen bond synchronization of the free molecules disappears in condensed media [42]. Actually in 1,2-butanediol three conformers were observed with the G'A all-trans heavy atom skeleton, which differ in the hydroxyl group orientation but always retain the intramolecular hydrogen bond. In 1,2-butanedithiol only one

G'A conformer was observed, but the fact that helium was required as carrier gas for the observation of six conformers in the alcohol suggests that additional conformations might be observable for the thiol with a carrier lighter than the neon used here.

The second observed conformation of 1,2-butanedithiol adopts a negative-gauche carbon skeleton and positive-gauche orientation of the two thiol groups denoted g'GG'g' in Table 1. Three gauche carbon skeletons were observed in 1,2-butanediol (aG'G'g, aG'Gg, g'GAa), but not a GG' configuration, which were predicted 2.8-4.8 kJ $mol^{-1}$ above the global minimum [25]. In 1,2-butanedithiol the second isomer was predicted with a lower conformational Gibbs energy of 0.9 kJ $mol^{-1}$, slightly higher than other GA and AA conformers. This fact suggest that either the conformational energy (quite similar between B3LYP and MP2) is not correctly predicted in the dithiol or that the observed populations have been modulated by conformational relaxation in the jet [43], as observed in the diol.

*Intramolecular hydrogen bonding*

The relative orientation of the two alcohol groups in 1,2-butanediol (r(O-H···O)=2.25 Å in Table S17, Supplementary information) and other poliols is considered a structural evidence of intramolecular hydrogen bonding and a determining factor in conformational stability [11]. By analogy, the orientation of the two thiol groups in 1,2-butanedithiol may indicate intramolecular S-H···S hydrogen bond interactions. In the global minimum a single S-H···S interaction seems favorable by the parallel orientation of the thiol groups and the favorable distance of *r*(S-H···S)=2.79 Å in Table 4. For the second conformer the thiol groups align antiparallel, exhibiting larger S-H···S distances (3.06 Å and 3.13 Å). The number of dithiols examined in the gas phase for comparison is yet scarce. While in 1,3-propanedithiol the different conformation to the alcohol is taken as evidence of no S-H···S intramolecular hydrogen bonding [11], in the case of 1,2-ethanedithiol [9] geometries similar to those of 1,2-butanedithiol are considered signatures of 1 and 2 S-H···S hydrogen bonds in conformers gGg and gGg', respectively. DFT calculations for

1,2-ethanedithiol gGg and gGg' in Tables S18 and S19 predict intramolecular hydrogen bond distances of *r*(S-H···S)=2.83 Å and 3.09 Å, respectively.

In order to verify the presence of intramolecular hydrogen bonding in the dithiols we used the NCIPLOT methodology [35], which can quantify and map tridimensionally the presence of non-covalent interactions based on a reduced gradient $s\ \left(=\frac{1}{2(3\pi^2)^{1/3}}\frac{|\nabla\rho|}{\rho^{4/3}}\right)$ of the electronic density $(\rho)$. We compare in Figure S1 (Supplementary information) the plots of the reduced gradient versus the signed electronic density $(=\mathrm{sign}(\lambda_2)\,\rho)$ using the second eigenvalue $(\lambda_2)$ of the electron density Hessian. The presence of plot minima at small negative values of the electronic density (more pronounced in the alcohol) suggests weak attractive interactions compatible with the presence of an intramolecular hydrogen bond in both 1,2-butanediol and the dithiol, but also regions of weak repulsive interactions in the two cases. The location of the intramolecular non-covalent interactions are shown in Figure 2.

## CONCLUSSION

We observed the rotational spectrum of 1,2-butanedithiol in the cm-wave region and detected two molecular conformations in a jet-cooled expansion using neon as carrier gas. The most stable conformation shares an all-trans carbon skeleton with the global minimum of 1,2-butanediol [25]. The orientation of the hydrogen bonds differs in the alcohol (aG'Ag) and the thiol (gG'Ag'), but in both cases the two polar groups synchronize the position of the hydrogen atoms to maintain an intramolecular hydrogen bond O-H···O or S-H···O, as observed in other poliols. A second isomer was observed for the dithiol, with a gauche carbon atom skeleton (g'GG'g'). Effective and substitution structures were determined for the global minimum of the dithiol from inertial data of seven distinct isotopologues, accurately characterizing the heavy atom skeleton. For the second less populated isomer three isotopologues were observed, which allowed the calculation of an effective structure. Weak intramolecular S-H···H hydrogen bonds operate in both conformers according to an NCIPLOT analysis. The conformational landscape derived from molecular orbital calculations with (B3LYP-D3(BJ)) DFT and (MP2) ab initio methods suggest multiple low-energy species, whose stability is considerably affected by the exchange of oxygen by sulfur. The observation of only two conformers in butanedithiol is small compared to other aliphatic open-chain molecules, indicating that conformational relaxation is effective in presence of neon in the expansion, so additional experiments with helium expansions would be necessary for further exploration of the conformational landscape. The structural predictions of B3LYP-D3(BJ) and MP2 satisfactorily reproduce the observed rotational constants (relative deviations of 0.3-1% in B3LYP-D3(BJ) and 0.2-2.4% in MP2 in Tables 1-3).

In conclusion, the present work progressed in the investigation of weak sulfur-centered hydrogen bonds in aliphatic dithiols, providing structural and energetic data that will be useful for future research on intermolecular complexes of the title compound.

**ACKNOWLEDGEMENTS**

Funding from the Spanish MICIU-FEDER (grant PGC2018-098561-B-C22) and JCyL (grant VA056G18) is gratefully acknowledged. M.J. and R. T. S. thank predoctoral contracts from the MECD and UVa, respectively. Y. J. thanks the China Scholarship for a predoctoral travel grant. The authors thank Dr. Jon Hougen for his contributions to science, generosity and personal lessons.

**AUTHOR CONTRIBUTIONS**

The manuscript was written through contributions of all authors. All authors have given approval to the final version of the manuscript.

**AUTHOR INFORMATION**

Corresponding author: Prof. Dr. Alberto Lesarri, lesarri@qf.uva.es, Tel.: +34-983-185895, Fax: +34-983-423013.

REFERENCES


[1] R. J. Cremlyn, An Introduction to Organosulfur Chemistry. Wiley: Chichester, 1996.

[2] G. Gilli, P. Gilli, The Nature of the Hydrogen Bond, IUC-Oxford University Press, Oxford, 2009.

[3] H. S. Biswal, Hydrogen Bonding Involving Sulfur: New Insights from Ab Initio Calculations and Gas Phase Laser Spectroscopy, in Noncovalent Forces (Ed.: S. Scheiner), Chap. 2, Springer Int. Pub., Switzerland, 2015.

[4] H. S. Biswal, S. Bhattacharyya, A. Bhattacherjee, S. Wategaonkar, Nature and strength of sulfur-centred hydrogen bonds: laser spectroscopic investigations in the gas phase and quantum-chemical calculations, Int. Rev. Phys. Chem. 34 (2015) 99–160.

[5] W. Caminati, J.-U. Grabow, Advancements in Microwave Spectroscopy, in Frontiers and Advances in Molecular Spectroscopy, Chapter 17, pp. 569–598, Elsevier, Amsterdam, 2018.

[6] M. Juanes, R. T. Saragi, W. Caminati, A. Lesarri, The Hydrogen Bond and Beyond: Perspectives for Rotational Investigations of Non-Covalent Interactions, Chem. Eur. J. 25 (2019) 11402–11411.

[7] M. Juanes, A. Lesarri, R. Pinacho, E. Charro, J. E. Rubio, L. Enríquez, M. Jaraíz, Sulfur Hydrogen Bonding in Isolated Monohydrates: Furfuryl Mercaptan versus Furfuryl Alcohol, Chem. Eur. J. 24 (2018) 6564–6571.

[8] a) M. Hayashi, H. Imaishi, K. Kuwada, Microwave Spectrum, Structure and Dipole Moment of Ethanethiol. I. Trans isomer, Bull. Chem. Soc. Japan 47 (1974) 2382–2388. b) R. E. Schmidt, C. R. Quade, Microwave spectrum of ethyl mercaptan, J. Chem. Phys. 62 (1975) 3864–3874. c) M. Hayashi, J. Nakagawa, K. Kuwada, Microwave Spectra and Molecular Structure of Gauche-Ethanethiol, Chem. Lett. (1975) 1267–1270. d) J. Nakagawa, K. Kuwada, M. Hayashi, Microwave Spectrum, Structure, Dipole Moment and Internal Rotation of Ethanethiol. II. Gauche isomer, Bull. Chem. Soc. Japan 49 (1976) 3420v3432.

[9] K.-M. Marstokk, H. Mollendal, Structural and Conformational Properties of 1,2-Ethanedithiol as Studied by Microwave Spectroscopy and Ab initio Calculations, Acta Chem. Scand. 51 (1997) 653-663.

[10] J. Nakagawa, M. Hayashi, Double Minimum Splitting in Gauche 1-Propanethiol by Microwave Spectrum, Chem. Lett. (1979) 1321–1322.

[11] A. Vigorito, C. Calabrese, E. Paltanin, S. Melandri, A. Maris, Regarding the torsional flexibility of the dihydrolipoic acid's pharmacophore: 1,3-propanedithiol, Phys. Chem. Chem. Phys. 19 (2017) 496–502.

[12] K.-M. Marstokk, H. Møllendal, Microwave Spectrum, Conformational Equilibria, Intramolecular Hydrogen Bonding and Centrifugal Distortion of 3-Butene-1-thiol, Acta Chem. Scand. 40a (1986) 402–411.

[13] G. C. Cole, H. Møllendal, J.-C. Guillemin, Microwave Spectrum of 3-Butyne-1-thiol: Evidence for Intramolecular S−H···π Hydrogen Bonding, J. Phys. Chem. A 110 (2006) 9370–9376.

[14] K.-M. Marstokk, H. Møllendal, A Microwave and Ab Initio Study of the Conformational Properties and Intramolecular Hydrogen Bonding of Cyclopropanemethanethiol, Acta Chem. Scand. 45 (1991) 354–360.

[15] H. Møllenda, S. Samdal, J.-C. Guillemin, Rotational Spectrum, Conformational Composition, Intramolecular Hydrogen Bonding, and Quantum Chemical Calculations of Mercaptoacetonitrile, a Compound of Potential Astrochemical Interest, J. Phys. Chem. A 120 (2016) 1992–2001.

[16] J. Zhang, X. Li, Q. Gou, G. Feng, Disulfide Bond in Diethyl Disulfide: A Rotational Spectroscopic Study, J. Phys. Chem. A 122 (2018) 5597–5601.

[17] J. Demaison, N. Vogt, R. T. Saragi, M. Juanes, H.-D. Rudolph, A. Lesarri, How flexible is the disulfide linker? A combined rotational–computational investigation of diallyl disulfide, Phys. Chem. Chem. Phys. 21 (2019) 19732–19736.

[18] J. Demaison, N. Vogt, R. T. Saragi, M. Juanes, H.-D. Rudolph, A. Lesarri, The S−S Bridge: A Mixed Experimental-Computational Estimation of the Equilibrium Structure of Diphenyl Disulfide, 20 (2019), 366–373.

[19] H. Møllendal, A. Konovalov, J.-C. Guillemin, Microwave Spectrum and Intramolecular Hydrogen Bonding of 2-Propene-1-selenol, J. Phys. Chem. A 113 (2009) 6342–6347.

[20] D. Petitprez, J. Demaison, G. Wlodarczak, J.-C. Guillemin, H. Møllendal, 3-Buteneselenol - The First Example of a Selenol with an Intramolecular Hydrogen Bond as Studied by Microwave Spectroscopy and Quantum Chemical Calculations, J. Phys. Chem. A 108 (2004) 1403–1408.

[21] H. Møllendal, R. Mokso, J.-C. Guillemin, A Microwave Spectroscopic and Quantum Chemical Study of 3-Butyne-1-selenol, J. Phys. Chem. A 112 (2008) 3053–3060.

[22] G. C. Cole, H. Møllendal, J.-C. Guillemin, Spectroscopic and Quantum Chemical Study of the Novel Compound Cyclopropylmethylselenol, J. Phys. Chem. A 110 (2006) 2134–2138.

[23] H. Møllendal, A. Konovalov, J.-C. Guillemin, Microwave Spectrum and Intramolecular Hydrogen Bonding of Propargyl Selenol, J. Phys. Chem. A 114 (2010) 5537–5543.
[24] a) I. A. Smirnov, E. A. Alekseev, V. I. Piddyachiy, V. V. Ilyushin, R. A. Motiyenko, 1,3-Propanediol millimeter wave spectrum: Conformers I and II, J. Mol. Spectrosc. 293-294 (2013), 33–37. b) O. Zakharenko, J.-B. Bossa, F. Lewen, S. Schlemmer, H. S. P. Müller, Millimeter and submillimeter wave spectroscopy of higher energy conformers of 1,2-propanediol, J. Mol. Spectrosc. 333 (2017), 23–26.
c) B. E. Arenas, S. Gruet, A. L. Steber, M. Schnell, A global study of the conformers of 1,2-propanediol and new vibrationally excited states, J. Mol. Spectrosc. 337 (2017), 9–16.
[25] A. Vigorito, C. Calabrese, S. Melandri, A. Caracciolo, S. Mariotti, A. Giannetti, M. Massardi, A. Maris, Millimeter-wave Spectroscopy and Modeling of 1,2-Butanediol, Astron. & Astrophys. 619 (2018) A140–1/9
[26] J. Paul, I. Hearn, B. J. Howard, Chiral recognition in a single molecule: a study of homo and heterochiral butan-2,3-diol by Fourier transform microwave spectroscopy, Mol. Phys. 105 (2007) 825-839.
[27] E. J. Cocinero, A. Lesarri, P. Écija, F. J. Basterretxea, J.-U. Grabow, J. A. Fernández, F. Castaño, Ribose Found in the Gas Phase, Angew. Chem. Int. Ed. 51 (2012) 3119–.
[28] E. J. Cocinero, A. Lesarri, P. Écija, Á. Cimas, B. G. Davis, F. J. Basterretxea, J. A. Fernández, F. Castaño, Free Fructose Is Conformationally Locked, J. Am. Chem. Soc. 135 (2013) 135, 2845–2852.
[29] S. T. Shipman, B. H. Pate in Handbook of High Resolution Spectroscopy (Eds.: M. Quack, F. Merkt), Wiley, New York, 2011, pp. 801–828.
[30] C. Pérez, S. Lobsiger, N. A. Seifert, D. P. Zaleski, B. Temelso, G. C. Shields, Z. Kisiel, B. H. Pate, Broadband Fourier transform rotational spectroscopy for structure determination: The water heptamer, Chem.Phys. Lett. 571 (2013), 1–15.
[31] N. A. Seifert, A. L. Steber, J. L. Neill, C. Pérez, D. P. Zaleski, B. H. Pate, A. Lesarri, The interplay of hydrogen bonding and dispersion in phenol dimer and trimer: structures from broadband rotational spectroscopy, Phys. Chem. Chem. Phys. 15 (2013) 11468–11477.
[32] S. Grimme, S. Ehrlich, L. Goerick, J. Comb. Chem. 32 (2011) 1456–1465.
[33] F. Weigend, R. Ahlrichs, Phys. Chem. Chem. Phys. 7(2005) 3297–3305.
[34] Gaussian 16, Revision C.01, M. J. Frisch, G. W. Trucks, H. B. Schlegel, G. E. Scuseria, M. A. Robb, J. R. Cheeseman, G. Scalmani, V. Barone, G. A. Petersson, H. Nakatsuji, X. Li, M. Caricato, A. V. Marenich, J. Bloino, B. G. Janesko, R. Gomperts, B. Mennucci, H. P. Hratchian, J. V. Ortiz, A. F. Izmaylov, J. L. Sonnenberg, D. Williams-Young, F. Ding, F. Lipparini, F. Egidi, J. Goings, B. Peng, A. Petrone, T. Henderson, D. Ranasinghe, V. G. Zakrzewski, J. Gao, N. Rega, G. Zheng, W. Liang, M. Hada, M. Ehara, K. Toyota, R. Fukuda, J. Hasegawa, M. Ishida, T. Nakajima, Y. Honda, O. Kitao, H. Nakai, T. Vreven, K. Throssell, J. A. Montgomery, Jr., J. E. Peralta, F. Ogliaro, M. J. Bearpark, J. J. Heyd, E. N. Brothers, K. N. Kudin, V. N. Staroverov, T. A. Keith, R. Kobayashi, J. Normand, K. Raghavachari, A. P. Rendell, J. C. Burant, S. S. Iyengar, J. Tomasi, M. Cossi, J. M. Millam, M. Klene, C. Adamo, R. Cammi, J. W. Ochterski, R. L. Martin, K. Morokuma, O. Farkas, J. B. Foresman, and D. J. Fox, Gaussian, Inc., Wallingford CT, 2016.
[35] J. Contreras-García, E. R. Johnson, S. Keinan, R. Chaudret, J.-P. Piquemal, D. N. Beratan, W. Yang, NCIPLOT: A Program for Plotting Noncovalent Interaction Regions, J. Chem. Theory Comput. 7 (2011) 625–632.
[36] B. H. Pate, L. Evangelisti, W. Caminati, Y. Xu, J. Thomas, D. Patteson, C. Pérez, M. Schnell, in Chiral Analysis, 2nd ed. (Ed.: P.L. Polavarapu), ch. 17, pp. 679-729, Elsevier, Amsterdam, 2018.
[37] H. M. Pickett, The Fitting and Prediction of Vibration-Rotation Spectra
with Spin Interactions, J. Mol. Spectrosc. 148 (1991) 371–377.
[38] H. D. Rudolph, J, Demaison in Equilibrium Molecular Structures: From Spectroscopy to Quantum Chemistry, 1st Edition (Eds: J. Demaison, J. E. Boggs, A. G. Csaszar), chap.5, pp. 125–158, CRC Press, Boca Ratón, FL, 2011.
[39] MOMSTRUC structural package available at: https://www.uni-ulm.de/~hrudolph/ (last accessed: November 2019).
[40] C. C. Costain, Further comments on the accuracy of rs substitution structures, Trans. Am. Cryst. Ass. 2 (1966) 157–164.
[41] J Demaison, H. D. Rudolph, When Is the Substitution Structure Not Reliable?, J. Mol. Spectrosc. 215 (2002) 78-84.
[42] C. Calabrese, P. Écija, I. Compañón, M. Vallejo-López, Á. Cimas, M. Parra, F. J. Basterretxea, J. I. Santos, J. Jiménez-Barbero, A. Lesarri, F. Corzana, E. J. Cocinero, Conformational Behavior of d-Lyxose in Gas and Solution Phases by Rotational and NMR Spectroscopies, J. Phys. Chem. Lett. 10 (2019) 3339-3345.

[43] P. D. Godfrey, R. D. Brown, Proportions of Species Observed in Jet Spectroscopy-Vibrational Energy Effects: Histamine Tautomers and Conformers, J. Am. Chem. Soc. 1998 (120), 10724-10732.

**Figure 1**. Microwave spectrum of 1,2-butanedithiol in the region 2-8 GHz (lower trace), and typical $^{34}S$ and $^{13}C$ transitions in natural abundance (4% and 1%). The upper spectral trace has been expanded by factors of 600 x (horizontal) and 20 x (vertical)

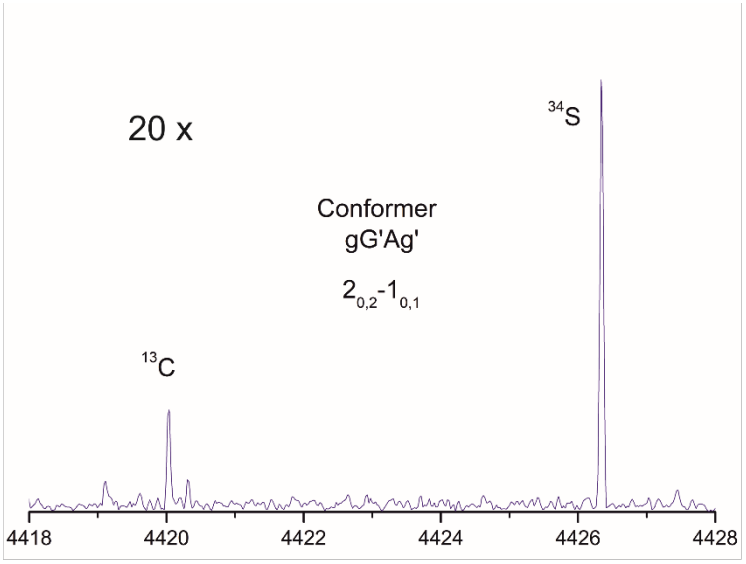


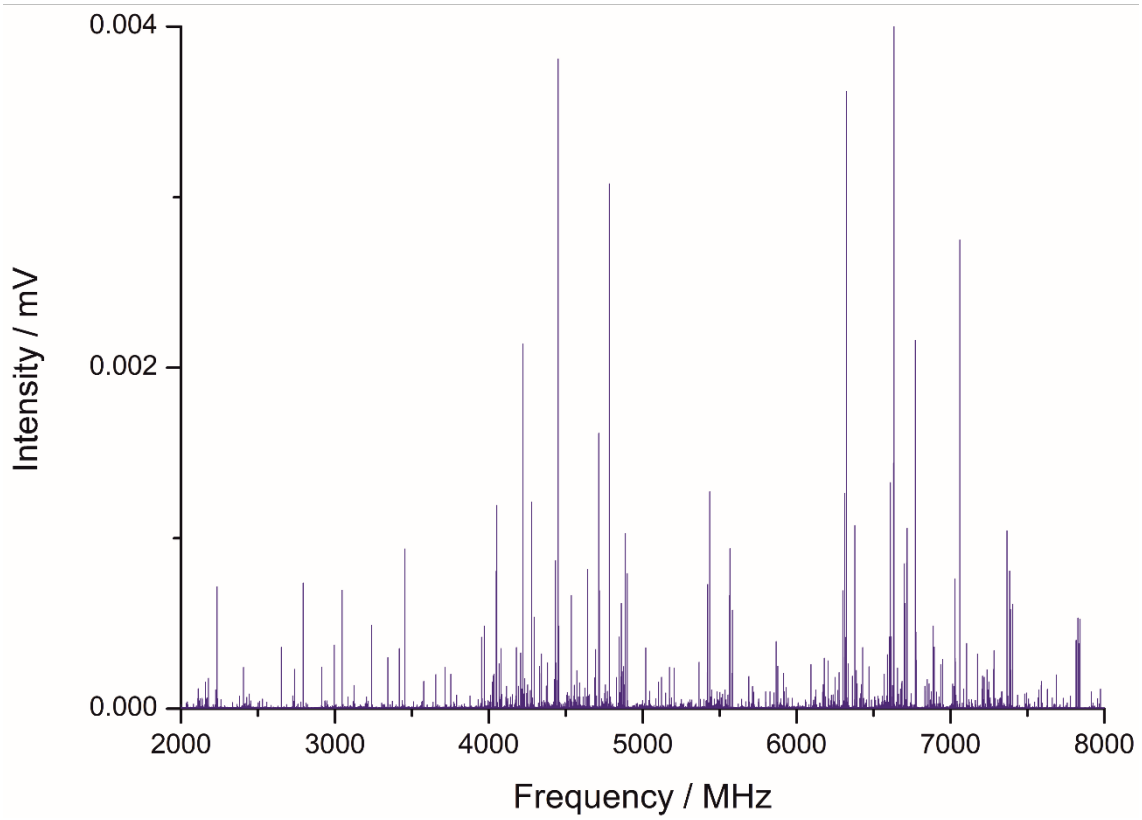

**Figure 2**. The observed conformers gG'Ag' (upper panel) and g'GG'g' (center panel) of 1,2-butanedithiol and comparison with the most stable conformer aG'Ag of 1,2-butanediol (lower panel). The molecular conformations include NCIPLOT maps of the non-covalent interactions, suggesting weak attractive (dark green) and repulsive (light green) interactions in the three cases (sgn($\lambda_2$) $r$ = -0.04 to 0.04 a.u., see Figure S1 in Supporting Information).

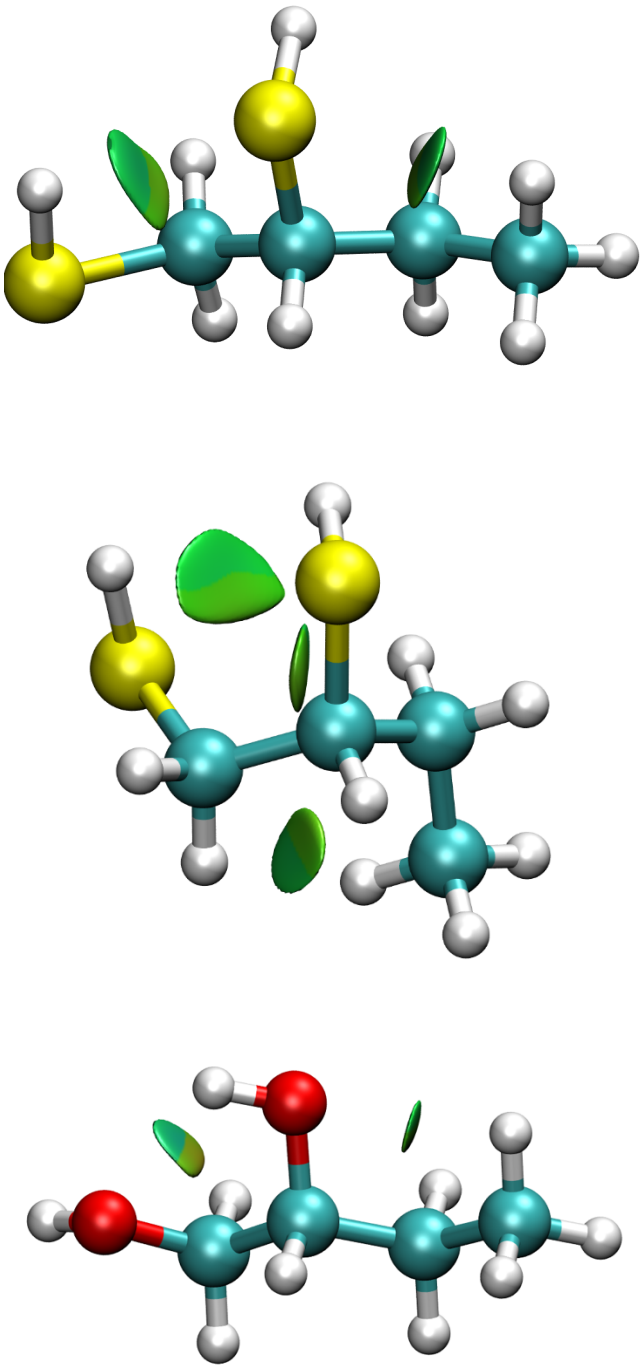

**Table 1**. Computational predictions for the most stable conformations of 1,2-butanedithiol (B3LYP-GD3BJ/def2TZVP and MP2/def2TZVP).

| | Theory[c] | | | | | | | |
|---|---|---|---|---|---|---|---|---|
| | **Conformer gG'Ag'** | Conformer g'GAg' | Conformer gAAg' | **Conformer g'GG'g'** | Conformer gG'G'g' | Conformer g'GAg | Conformer gAGg' | Conformer gG'Gg' |
| $A$[a] | 3610.67/3681.95[d] | 2922.91/2961.61 | 2950.30/2992.95 | 2065.32/2124.41 | 2485.79/2524.33 | 2904.33/2935.18 | 3031.01/3094.33 | 3068.57/3090.68 |
| $B$ | 1236.61/1249.19 | 1439.24/1461.04 | 1296.09/1313.02 | 1929.37/1947.54 | 1523.28/1544.46 | 1453.66/1476.99 | 1351.47/1375.69 | 1372.23/1393.03 |
| $C$ | 989.74/1002.57 | 1124.46/1144.53 | 956.23/969.73 | 1153.44/1180.01 | 999.13/1012.90 | 1133.73/1152.92 | 1046.23/1070.01 | 1057.13/1073.04 |
| $D_J$ / kHz | 0.0654/0.0658 | 0.1687/0.1730 | 0.0996/0.1036 | 1.4043/1.2227 | 7.6420/0.7448 | -8.0493/0.1742 | 0.0579/0.0597 | 0.1253/0.1342 |
| $D_{JK}$ / kHz | 0.7726/0.7977 | 0.7360/0.6950 | 0.3199/0.2463 | -2.3502/-2.0411 | -1.0074/-0.9795 | -3.1906/0.6574 | 3.7535/3.0658 | 0.5193/0.4644 |
| $D_K$ / kHz | 3.1012/3.0646 | 1.1531/1.1919 | 1.8631/2.1611 | 1.0738/0.9475 | 0.2898/0.2818 | -1.0063/1.2952 | -2.2469/-1.4727 | 2.1605/2.4238 |
| $d_1$ / kHz | -0.0087/-0.0084 | -0.0292/-0.0292 | -0.0362/-0.0375 | 0.2831/-0.0451 | -0.3683/-0.3518 | -0.7049/-0.0337 | -0.0175/-0.0139 | -0.0310/-0.0353 |
| $d_2$ / kHz | -0.0036/-0.0036 | -0.0090/-0.0089 | -0.0087/-0.0083 | -0.3596/0.3024 | -0.1377/-0.1303 | -0.6699/-0.0101 | -0.0324/-0.0255 | -0.0058/-0.0059 |
| $\mu_a$ / D | 1.68/1.68 | 0.45/-0.44 | 0.15/0.14 | 0.21/0.02 | 2.08/2.08 | 0.51/0.86 | 0.00/0.04 | 1.87/1.83 |
| $\mu_b$ / D | 1.06/1.00 | 0.74/-0.68 | 0.24/0.23 | 1.08/-1.03 | 0.55/0.50 | 0.17/0.06 | 0.30/0.27 | 1.18/1.13 |
| $\mu_c$ / D | 1.08/1.11 | 0.77/0.71 | 0.17/0.14 | 0.52/0.46 | 0.97/1.00 | 1.73/1.72 | 0.17/0.19 | 0.36/0.43 |
| $\Delta E_{ZPE}$ / kJ mol$^{-1}$ [b] | 0.00/0.00 | 0.20/0.71 | 0.63/1.07 | 0.66/0.41 | 2.26/2.13 | 2.79/2.71 | 3.22/3.62 | 3.86/4.39 |
| $\Delta G$ / kJ mol$^{-1}$ | 0.20/0.00 | 0.42/0.82 | 0.00/0.17 | 0.90/0.92 | 2.23/1.89 | 2.71/2.36 | 2.89/3.62 | 4.49/4.82 |

[a]Rotational constants ($A$, $B$, $C$), Watson's S-reduction centrifugal distortion constants ($D_J$, $D_{JK}$, $D_K$, $d_1$, $d_2$) and electric dipole moments ($\mu_\alpha$, α = a, b, c). [b]Relative energies corrected with the zero-point energy (ZPE) and Gibbs energy ($\Delta G$, 298K, 1 atm). [c]The conformers observed experimentally are marked in bold typeface. [d]B3LYP-GD3BJ (left column) and MP2 (right column) calculations (basis set def2TZVP).

**Table 2**. Rotational parameters for the most intense conformer 1 of 1,2-butanedithiol, including the parent species and all carbon and sulfur monosubstituted species.

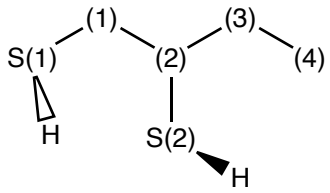


| | Conformer 1 = gG'Ag' | | | | | | |
|---|---|---|---|---|---|---|---|
| | Parent | $^{34}$S(1) | $^{34}$S(2) | $^{13}$C(1) | $^{13}$C(2) | $^{13}$C(3) | $^{13}$C(4) |
| *A* / MHz[a] | 3646.9937(20) | 3641.1026(30) | 3532.5314(43) | 3621.7914(29) | 3644.3521(51) | 3616.32(25) | 3630.4502(72) |
| *B* / MHz | 1240.40699(23) | 1206.13130(74) | 1238.5810(10) | 1237.48180(63) | 1239.9087(11) | 1231.8891(12) | 1214.3670(15) |
| *C* / MHz | 994.42254(23) | 972.17730(72) | 984.5632(10) | 991.65340(56) | 994.0070(10) | 987.0757(12) | 977.0784(14) |
| $D_J$ / kHz | [ 0.] | [ 0.] | [ 0.] | [ 0.] | [ 0.] | [ 0.] | [ 0.] |
| $D_{JK}$ / kHz | 0.767(23) | [0.767] | [0.767] | [0.767] | [0.767] | [0.767] | [0.767] |
| $D_K$ / kHz | 2.93(42) | [2.93] | [2.93] | [2.93] | [2.93] | [2.93] | [2.93] |
| $d_1$ / kHz | [ 0.] | [ 0.] | [ 0.] | [ 0.] | [ 0.] | [ 0.] | [ 0.] |
| $d_2$ / *k*Hz | -0.00634(74) | [-0.00634] | [-0.00634] | [-0.00634] | [-0.00634] | [-0.00634] | [-0.00634] |
| *N*[b] | 48 | 11 | 11 | 7 | 7 | 6 | 7 |
| $\sigma$ / kHz | 5.4 | 3.3 | 5.4 | 2.5 | 3.8 | 3.9 | 5.3 |

[a]Rotational constants (*A*, *B*, *C*), Watson's S-reduction centrifugal distortion constants ($D_J$, $D_{JK}$, $D_K$, $d_1$, $d_2$). [b]Number of transitions (*N*) and rms deviation ($\sigma$) of the fit. [c]Standard errors in parentheses in units of the last digit. [d]Values in square brackets were kept fixed in the fit.

**Table 3.** Rotational parameters for isomer CS2 of 1,2-butanedithiol. including the parent species and the two $^{34}S$ monosubstituted species in natural abundance.

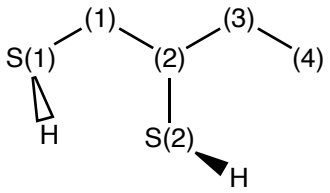


| | Conformer 2 = g'GG'g' | | |
|---|---|---|---|
| | Parent | $^{34}S(1)$ | $^{34}S(2)$ |
| *A* / MHz[a] | 2073.4247(11) | 2064.1416(19) | 2059.2935(18) |
| *B* / MHz | 1954.09725(87) | 1902.3933(58) | 1908.0361(55) |
| *C* / MHz | 1164.70044(60) | 1143.9816(11) | 1143.9313(10) |
| $D_J$ / kHz | [ 0.] | [ 0.] | [ 0.] |
| $D_{JK}$ / kHz | 1.270(51) | [1.270] | [1.270] |
| $D_K$ / kHz | -0.546(52) | [-0.546] | [-0.546] |
| $d_1$ / kHz | -0.196(11) | [-0.196] | [-0.196] |
| $d_2$ / *k*Hz | -0.1033(51) | [-0.1033] | [-0.1033] |
| *N*[b] | 34 | 6 | 6 |
| $\sigma$ / kHz | 5.9 | 4.0 | 3.7 |

[a]Rotational constants (*A*, *B*, *C*), Watson's S-reduction centrifugal distortion constants ($D_J$, $D_{JK}$, $D_K$, $d_1$, $d_2$). [b]Number of transitions (*N*) and rms deviation ($\sigma$) of the fit. [c]Standard errors in parentheses in units of the last digit. [d]Values in square brackets were kept fixed in the fit.

**Table 4**. Molecular structure of conformer gG'Ag' of 1,2-butanedithiol.

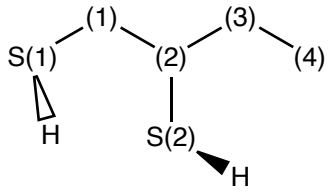


| | gG'Ag' | | |
|---|---|---|---|
| | Effective | Substitution | DFT |
| | $r_0$ | $r_s$ | $r_e$ |
| Fitted parameters | | | |
| *r*(S(1)-C(1)) / Å | 1.821(6)[a] | 1.826(4)[b] | 1.821[c] |
| *r*(C(1)-C(2)) / Å | 1.507(31) | 1.500(7) | 1.528 |
| *r*(C(2)-S(2)) / Å | 1.825(28) | 1.805(10) | 1.838 |
| *r*(C(2)-C(3)) / Å | 1.548(34) | 1.567(7) | 1.531 |
| *r*(C(3)-C(4)) / Å | 1.530(14) | 1.528(5) | 1.524 |
| ∠(S(1)-C(1)-C(2)) / deg | 114.8(14) | 113.7(4) | 115.4 |
| ∠(C(1)-C(2)-S(2)) / deg | 113.0(18) | 114.3(13) | 111.8 |
| ∠(C(1)-C(2)-C(3)) / deg | 111.0(2.4) | 109.5(6) | 111.2 |
| ∠(C(2)-C(3)-C(4)) / deg | 114.8(1.5) | 114.6(5) | 114.6 |
| τ(S(1)-C(1)-C(2)-S(2)) / deg | -64.9(28) | -64.9(22) | -65.1 |
| τ(S(1)-C(1)-C(2)-C(3)) / deg | 168.3(11) | 168.5(5) | 168.0 |
| τ(C(1)-C(2)-C(3)-C(4)) / deg | -171.9(18) | -171.9(5) | -171.7 |
| Derived values | | | |
| *r*(S(1)-H) / Å | 1.344(10) | | 1.344 |
| *r*(S(2)-H) / Å | 1.345(13) | | 1.345 |
| *r*(S(1)-H···S) / Å | 2.775(7) | | 2.788 |
| ∠(C(1)-S(1)-H) / deg | 95.8(6) | | 95.8 |
| ∠(C(2)-S(2)-H) / deg | 96.0(23) | | 96.0 |
| τ(H-S(1)-C(1)-C(2)) / deg | 57.3(19) | | 57.3 |
| τ(H-S(2)-C(2)-C(1)) / deg | 67.4(32) | | -67.4 |

[a]Standard errors in parentheses in units of the last digit for a fit of 21 datapoints to 12 structural parameters. Standard errors do not include additional uncertainties associated to the fitting model. [b]Costain errors proportional to the coordinate magnitude. [c]B3LYP-D3(BJ)/def2TZVP.

**Table 5**. Molecular structure of conformer g'GG'g' of 1,2-butanedithiol.

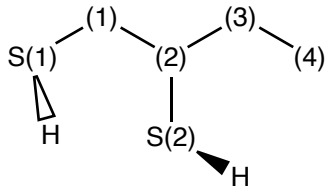


| | g'GG'g | |
|---|---|---|
| | Effective | DFT |
| | $r_0$ | $r_e$ |
| Fixed parameters | | |
| r(S(1)-C(1)) / Å | [1.825][a] | 1.825[d] |
| r(C(1)-C(2)) / Å | [1.531] | 1.531 |
| r(C(2)-S(2)) / Å | [1.836] | 1.836 |
| r(C(2)-C(3)) / Å | [1.529] | 1.529 |
| r(C(3)-C(4)) / Å | [1.528] | 1.528 |
| ∠(S(1)-C(1)-C(2)) / deg | {115.6}[b] | 115.9 |
| ∠(C(1)-C(2)-S(2)) / deg | {111.1} | 112.0 |
| ∠(C(1)-C(2)-C(3)) / deg | {114.6} | 114.8 |
| ∠(C(2)-C(3)-C(4)) / deg | {111.7} | 113.7 |
| Fitted parameters | | |
| τ(S(1)-C(1)-C(2)-S(2)) / deg | -69.193(14)[c] | -69.2 |
| τ(S(1)-C(1)-C(2)-C(3)) / deg | 59.347(51) | 59.3 |
| τ(C(1)-C(2)-C(3)-C(4)) / deg | 57.520(93) | 57.5 |
| Derived values | | |
| r(S(1)-H) / Å | 1.343(4) | 1.343 |
| r(S(2)-H) / Å | 1.344(4) | 1.344 |
| r(S(1)-H···S) / Å | 3.027(3) | 3.061 |
| r(S(2)-H···S) / Å | | 3.134 |
| ∠(C(1)-S(1)-H) / deg | 96.4(1) | 96.4 |
| ∠(C(2)-S(2)-H) / deg | 96.3(1) | 96.4 |
| τ(H-S(1)-C(1)-C(2)) / deg | -73.2(1) | -73.2 |
| τ(H-S(2)-C(2)-C(1)) / deg | -77.9(1) | -77.9 |

[a]Parameters in square brackets were kept fixed to the B3LYP values. [b]Parameters in curly braces were kept fixed to an initial fit of the four valence angles [c]Standard errors in parentheses in units of the last digit for a fit of 9 moments of inertia to 3 dihedrals. Standard errors do not include additional uncertainties associated to the fitting model. [d]B3LYP-D3(BJ)/def2TZVP.